Prostanoid Receptor Gene Expression Profile in Human Trabecular Meshwork: A Quantitative Real-Time PCR Approach

Willem Kamphuis,[1] *Andrea Schneemann,*[1] *Luc M. van Beek,*[2] *August B. Smit,*[3] *Philip F. J. Hoyng,*[1] *and Eisuke Koya*[3]

Purpose. To assess the expression pattern of prostanoid receptor–encoding genes in trabecular meshwork (TM) of human donor eyes.

Methods. Disposed human donor eyes ($n = 10$) were obtained from the Cornea Bank, Amsterdam. The TM was dissected from the scleral tissue and homogenized in lysis buffer, and total RNA was isolated. The RNA was converted into cDNA and used as a template for noncompetitive quantitative real-time polymerase chain reaction (PCR) using green fluorescent dye to quantify the accumulation of double-stranded PCR product. Specific primers for four housekeeping genes and DP, EP_1, EP_2, EP_3, EP_4, FP, IP, and TP receptor–encoding transcripts were developed and tested for their efficiency.

Results. The characterized expression profile was highly reproducible in all samples, with the EP_2 receptor–encoding transcript in the highest abundance, followed by FP, TP, IP, and EP_4 at levels that were approximately 10 to 15 times lower than that of the EP_2 subtype. DP and EP_3 were at the lowest levels, which were, on average, 45 times and 228 times lower than EP_2, respectively.

Conclusions. These data show that all prostanoid receptors are expressed at different levels in human TM tissue. Because the gene expression of the EP_2 receptor is, on average, 15 times more abundant than that of the EP_4 receptor, it may be expected that the increase in flow and cAMP levels in response to the activation of the EP receptors by application of prostaglandin E_1 (PGE_1), is primarily mediated by the EP_2 receptor. These data should be considered when designing prostanoid receptor mimetics intended to enhance the aqueous humor outflow through the TM and Schlemm's canal. (*Invest Ophthalmol Vis Sci.* 2001;42:3209–3215)

The relationship between intraocular pressure (IOP) and the process of retinal ganglion cell loss in glaucoma remains to be established, but an increased pressure is considered to be at least a significant risk factor for the impairment of the visual field. Elevated IOP levels may result from reduced outflow of aqueous humor through the trabecular meshwork (TM) and Schlemm's canal,[1,2] for which a mechanical obstruction may be the cause, but, in most cases, the reason for the functional impairment of outflow is unclear. To regulate elevated IOP levels, prostaglandin (PG) receptor agonists are frequently applied as a means of pharmacologic intervention.[3,4] For instance, the prostaglandin $PGF_{2\alpha}$ analogue latanoprost, has been shown to reduce the IOP by 27% to 35% by facilitating uveoscleral outflow.[3,5–7] Furthermore, in diverse experimental models, agonists for other prostanoid receptors have also been shown to reduce the IOP.[8–12]

Prostaglandins are arachidonic acid metabolites that have an important auto- and paracrine role in both physiological and pathophysiological processes.[13] Human TM cells in culture produce PGE_2 and $PGF_{2\alpha}$, and these prostaglandins may therefore play a role in IOP regulation.[14] Prostaglandins exert their effects through activation of different prostaglandin receptors, which are classified according to their endogenous ligands: DP, EP, FP, IP, and TP receptors. The EP receptor is further subdivided into EP_1, EP_2, EP_3, and EP_4 subtypes, with additional heterogeneity created by alternative splicing of the EP_3 transcript.[15] Each of these receptors has been cloned, expressed, and characterized.[13]

Recently, we reported that the flow through the TM of perfused human anterior segments is increased by 26% after application of PGE_1. The simultaneous increase of cAMP levels in the perfusate indicates that the effect of PGE_1 is mediated through an adenyl cyclase–dependent pathway activated by either EP_2 or EP_4 receptors present in the TM.[16] Various techniques have shown the presence of prostanoid receptors in the TM. Immunoreactivity against EP_3 and EP_4 receptors was localized in porcine TM.[17] FP receptor mRNA and protein were found in monkey,[18] and human TM.[19] Furthermore, in isolated bovine TM strips, AH13205, an EP_2 receptor agonist, had a relaxant effect that may be related to the described effect of PGE_1 on outflow.[16,20] In contrast, activation of TP receptors induces a contraction of TM.[20,21]

The purpose of the present study was to determine, using reverse transcription (RT)–quantitative polymerase chain reaction (PCR), which of the known prostanoid receptor–encoding genes is expressed in the human TM and to assess the relative level of the genes' expression.

Materials and Methods

TM Tissue

Human donor eyes, rejected for corneal transplantation because of corneal opacities or abnormalities of corneal endothelium, were obtained from the Cornea Bank, Amsterdam. No animals were used in this study, and no donor details were revealed other than age, sex, and time of death. Details about the donors ($n = 10$) are given in Table 1. TM tissue was obtained as follows: The eye was bisected at the equator and the lens and iris were removed from the anterior segment. The seg-

From the [1]Glaucoma Research Group, Netherlands Ophthalmic Research Institute (NORI)-KNAW, and the [3]Department of Molecular and Cellular Neurobiology, Research Institute of the Neurosciences Vrije Universiteit, Graduate School of the Neurosciences, Amsterdam, The Netherlands; and the [2]Department of Ophthalmology, Leiden University Medical Centre, The Netherlands.

Presented in part at the annual meeting of the Association for Research in Vision and Ophthalmology, Fort Lauderdale, Florida, May 2000.

Submitted for publication December 20, 2000; revised July 6, 2001; accepted August 13, 2001.

Commercial relationships policy: N.

The publication costs of this article were defrayed in part by page charge payment. This article must therefore be marked "*advertisement*" in accordance with 18 U.S.C. §1734 solely to indicate this fact.

Corresponding author: Willem Kamphuis, Netherlands Ophthalmic Research Institute, Meibergdreef 47, 1105 BA Amsterdam, The Netherlands. w.kamphuis@ioi.knaw.nl

TABLE 1. Details on Studied Donors

Sample	Donor Age/ Sex	ENT (h.min)	PMT (h.min)
1	68 F	5.50	22.50
2	75 M	5.00	23.30
3	70 M	3.55	20.55
4	54 M	6.35	9.45
5	63 F	10.45	15.15
6	70 M	7.15	9.45
7	69 F	8.45	30.00
8	79 F	4.40	17.40
9	66 M	7.30	20.00
10	72 M	6.30	19.00

ment was placed in a dish with the inner side up, and the surface over the TM was carefully wiped clean from adherent uveal tissue if still present. Under a dissecting microscope and using fine forceps, TM tissue strips were gently pulled from the corneoscleral cap. To verify whether this preparation procedure yielded clean TM tissue samples, some specimens of the corneoscleral cap were prepared for histologic inspection before and after isolation of the TM. Tissue was fixed in 4% paraformaldehyde in 0.1 M phosphate buffer (pH 7.2), cryoprotected with 30% sucrose in buffer, and frozen. Cryosections were cut and stained with hematoxylin-eosin for light-microscopic inspection.

cDNA from Human TM

Isolated TM tissue was homogenized, and total RNA was isolated by a single-step method, based on guanidine thiocyanate extraction, according to the manufacturer's instructions (Ultraspec; Biotecx Laboratories, Inc., Houston, TX). The isolated RNA was dissolved in a volume of 10 μl diethylpyrocarbonate-treated water. In a series of preliminary trials, the concentration of RNA was spectrophotometrically determined and was found to be on the order of 1 to 2 μg total RNA per isolated TM. To enhance the yield of total RNA, 20 μg yeast transfer (t)RNA was added to facilitate precipitation of the RNA. Because of the limited amount of RNA, the total yield of RNA was transcribed immediately into cDNA without quantification of the RNA concentration. Total RNA was reverse transcribed to cDNA using 100 ng of random primers and 200 U reverse transcriptase (Superscript RT; Life Technologies, Gaithersburg, MD) for 1 hour at 37°C. The cDNA (final volume, 50 μl in 10 mM Tris and 1 mM EDTA) was stored at −20°C until analysis.

A series of PCRs was performed on TM cDNAs with an intron-spanning primer pair for actin and quantitative real-time PCR–dedicated primers for the detection of the eight different prostanoid receptors. Primer pairs were designed on computer (Primer Express software; Applied Biosystems, Inc., Nieuwekerk aan de IJssel, The Netherlands). The length of the amplicons was kept as close as possible to 80 bp, and the melting temperature of the primers was set at 58°C to 60°C.[22] Details of the primers and the GenBank Accession Numbers are given in Table 2 (GenBank is provided in the public domain by the National Center for Biotechnology Information, Bethesda, MD, and is available at http://www.ncbi.nlm.nih.gov/genbank/). Specificity was checked in a BLAST search. For the EP_1, EP_3, FP, and TP receptors, alternative splicing has been described in the C-terminal region,[13] and primer design was therefore avoided in these regions. The conventional end-point PCR for β-actin was performed under the following conditions: annealing at 60°C, elongation at 74°C, and denaturing at 94°C, at 90 seconds for each step. Mg^{2+} concentration (1.5 mM), and 0.75 U *Taq* DNA polymerase (Qiagen-Westburg, Leusden, The Netherlands). The resultant PCR products were analyzed by agarose gel electrophoresis, and single bands of the anticipated size were found. For control purposes, mock cDNA samples without total RNA were prepared and subjected to PCR amplification. These samples yielded no PCR products.

Quantitative Real-Time PCR

Principles of Quantitative Real-Time PCR. The quantitative assessment of mRNA levels is performed using a detection system (Prism 7700 Sequence Detection System; Applied Biosystems Inc.) dedicated to the real-time monitoring of nucleic acid green dye fluorescence (SYBR Green I; Applied Biosystems Inc.). This dye is added to the PCR mixture and is fluorescent only when bound to double-stranded (ds)DNA, allowing measurement of the progressive accumulation of the specifically amplified product in the course of the PCR. A passive reference dye (ROX) is included in the PCR buffer providing an internal reference to which the fluorescent green dsDNA complex signal is normalized. This reference dye allows a correction for fluorescent fluctuations caused by non-PCR–related variations in concentration or volume.

During PCR amplification, the number of molecules synthesized (X_n) depends on the number of template molecules present at the start of the reaction (X_0), the reaction efficiency (E; ideally equal to 2), and the number of amplification rounds (n): $X_n = X_0 \cdot E^n$. In quantitative real-time PCR, the parameter cycle threshold (C_t) is defined as the fractional cycle number at which the green fluorescence passes the statistically significant level of 10 times the SD of the baseline emission during the first 10 cycles of the PCR. This point is reached during the exponential phase of amplification and is not affected by accumulated PCR product or the reaction components', such as dNTPs, becoming limited. The number of molecules synthesized at C_t is constant (C) despite different starting amounts[23]: $X_{C_t} = X_0 \cdot E^{C_t} \leftrightarrow X_0 = C \cdot E^{-C_t}$.

TABLE 2. GenBank Accession Code, Sequence of PCR Primer Pairs, and Anticipated Size of the Amplified Product for the Prostanoid Receptor Types and Housekeeping Genes

Receptor Subtype	Accession Code	Upstream Primer	Downstream Primer	Amplicon Length (bp)
actin	XM010801	CTGGAGAAGAGCTATGAGCTG	ATCTCCTTCTGCATCCTGTC	245
DP	U31332	TCTGCGCGCTACCTTTCATG	TCCTCGTGGACCATCTGGATA	85
EP_1	L22647	GATGGTGGGCCAGCTTGTC	GCCACCAACACCAGCATTG	72
EP_2	U19487	GTGCTGACAAGGCACTTCATGT	TGTTCCTCCAAAGGCCAAGTAC	87
EP_3	U13214	AAGGCCACGGCATCTCAGT	TGATCCCCATAAGCTGAATGG	76
EP_4	NM000958	CTTGGAGGCAGGAATTTGCTT	AAAGTCCTCAGTGAGGTGGTGTCT	96
FP	L24470	GCACATTGATGGGCAACTAGAA	GCACCTATCATTGGCATGTAGCT	90
IP	L29016	GCCGATCAGCTGCTGTTTCT	TTTCCTCTGTCCCTCACTCTCTTC	74
TP	D38081	ACGGAGAAGGAGCTGCTCATC	GCGGCGGAACAGGATATACA	84
GAPDH	M33197	TGCACCACCAACTGCTTAGC	GGCATGGACTGTGGTCATGA	87
β-actin	XM004814	GCTCCTCCTGAGCGCAAG	CATCTGCTGGAAGGTGGACA	75
HPRT	M31642	ATGGGAGGCCATCACATTGT	ATGTAATCCAGCAGGTCAGCAA	77
MHC class 1	BC004489	CACACCTCTCCTTTGTGACTTCAA	CCACCTCCTCACATTATGCTAACA	98

To facilitate presentation of the results on absolute amounts, we set C at 10^{10}.

Preliminary experiments were performed to establish the amplification efficiency (E) for each of the primer pairs, to allow a direct comparison of the expression levels of the different prostaglandin receptor genes.[23] A dilution range in water of a cDNA sample, prepared by pooling a fraction of the cDNAs of all individual samples included in this study, was subjected to PCR. C_t is related to the logarithm of the dilution factor, and the slope of the best-fit line is a measure for the reaction efficiency $E = 10^{-(1/\text{slope})}$ according to the manufacturer's instructions. These preliminary experiments were also performed to determine the optimal dilution of the cDNA to position the C_t between 15 and 30 cycles, as recommended by the manufacturer.

To correct for differences in cDNA load between the different TM samples, the target PCR may be normalized to a reference PCR, involving a selected endogenous housekeeping gene. From the C_t obtained from the individual donors, E^{-C_t} is calculated for target and reference. When the PCR reaches C_t, the number of amplified molecules for the target PCR and reference PCR are equal: $X_{C_t} = X_{0,\text{target}} \cdot E^{-C_{t,\text{target}}} = X_{0,\text{reference}} \cdot E^{-C_{t,\text{reference}}}$. From this, it follows that the ratio of the number of cDNA target molecules over the number of cDNA reference molecules at starting conditions: $X_{0,\text{target}}/X_{0,\text{reference}} = E^{-C_{t,\text{target}}}/E^{-C_t}$.[23]

Detection of Prostanoid Receptor Expression by Quantitative Real-Time PCR. The final reaction conditions were in 20 μl 1× fluorescent green dye PCR buffer (SYBR Green I; Applied Biosystems Inc.), 3 mM $MgCl_2$, 200 μM dATP, 200 μM dGTP, 200 μM dCTP, 400 μM dUTP, 0.5 U *Taq* polymerase (Ampli*Taq* Gold; Roche Molecular Systems Inc., Mannheim, Germany), 0.2 U uracil-*N*-glycosylase (UNG, AmpErase; Roche Molecular Systems Inc.), 6 pmol primers, and 0.375 μl cDNA, in a total volume of 20 μl. An initial step of 50°C for 2 minutes was used for AmpErase incubation followed by 10 minutes at 95°C to inactivate the AmpErase and to activate the *Taq* polymerase. Cycling conditions were: melting step at 95°C for 15 seconds and annealing-extension at 59°C for 1 minute, with 43 cycles. All reactions were performed at least in duplicate, and a maximum difference of 0.3 cycles between the C_t of the duplicate samples was considered acceptable. When this criterion was not fulfilled, the PCR was repeated. Nontemplate controls were included for each primer pair to check for significant levels of any contaminants. These samples always resulted in a difference of at least eight cycles of the C_t, compared with the template-containing samples.

The samples were subjected to a series of PCRs against four different housekeeping genes. The analyses of these data provide information on the influence of age, enucleation time, postmortem time, and the variation in total amount of cDNA. Subsequently, the samples were analyzed in PCRs, performed in parallel on 96-well plates against the prostaglandin receptors and β-actin gene, which was selected as the reference gene. Data are presented as absolute amount $C \cdot E^{-C_t}$ with $C = 10^{10}$. The ratio of the prostaglandin subtypes over β-actin ($E^{-C_{t,\text{target}}}/E^{-C_{t,\beta\text{-actin}}}$) was calculated to account for variability in the initial concentration of the total RNA and the conversion efficiency of the RT step.

Results

The total number of studied donors was 10 (6 male and 4 female). Mean age of the donors was 68.6 years (range, 54–79). The mean interval between time of death and enucleation of the eyes (ENT) was 6.40 hours (range, 3.55–10.45); the mean interval between time of death and start of RNA isolation in the laboratory (PMT) was 18.50 hours (range, 9.45–30). Details are given in Table 1.

Histologic examination of the isolated TM tissue and of the scleral cap after removing the TM tissue showed that most of the uveal, corneoscleral, and juxtacanicular regions were removed as illustrated in Figure 1. The scleral lining of Schlemm's canal was not isolated nor were parts of the anterior nonfiltering region of the TM near Schwalbe's line.

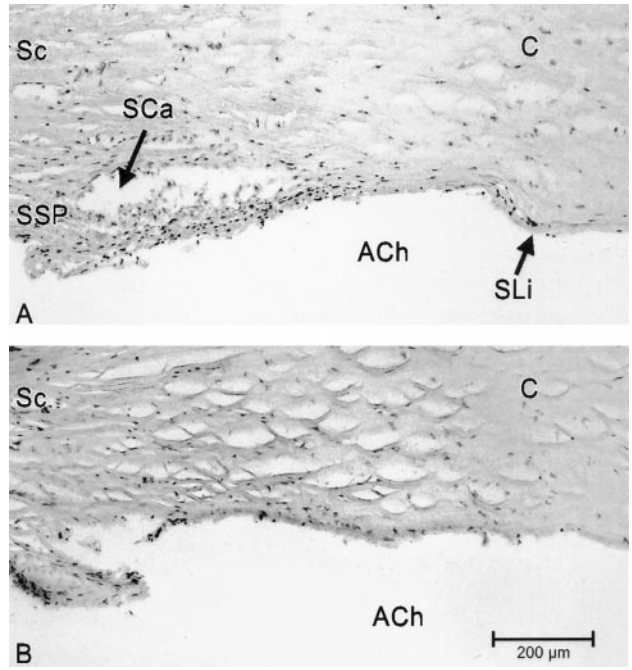

Figure 1. Photomicrograph of cryosections from the corneoscleral cap, with intact TM (**A**) and after isolation (**B**). The relatively large diameter of Schlemm's canal and the loose arrangement of the trabecular lamellae in the donor tissue may be because immersion fixation was used, and thus the normally present IOP was lost.[35] ACh, anterior chamber; C, cornea; Sc, sclera; SSP, scleral spur; SCa, Schlemm's canal; and SLi, Schwalbe's line. Bar, 200 μm.

In a preliminary series of RT-PCR experiments on cDNA samples prepared from isolated total RNA from TMs, the scores for each transcript were found to be erratic (data not shown). We reasoned that a possible explanation for the inconsistent results was a low yield of total RNA. To improve the amount of isolated RNA, tRNA was added as a precipitation carrier during the isolation procedure. As a result, the amount of amplified product increased for all prostanoid receptors and a consistent PCR pattern was observed. All 10 cDNA samples to be analyzed by quantitative real-time PCR, were first subjected to an actin-specific PCR with intron-spanning primers. All cases showed a single amplification product, which confirmed the absence of contaminating genomic DNA. The results are shown in Figure 2. The specific amplification products of prostanoid receptors that could be obtained from a cDNA sample, prepared by pooling a fraction of the cDNAs of all individual samples included in this study, are presented in Figure 2. Moreover, the real-time detection of dsDNA allows construction of a dissociation curve at the end of the PCR run by ramping the temperature of the sample from 60°C to 95°C while continuously collecting fluorescence data. The curves of the melting profiles of prostanoid receptors and housekeeping genes did not reveal an accumulation of primer dimers (data not shown).

The selection of the housekeeping gene to be used as the reference gene in a quantitative real-time PCR approach is a matter of ongoing debate.[22] We set out to test four different housekeeping genes that are often used for normalization[22]: glyceraldehyde-3-phosphate dehydrogenase (GAPDH), β-actin, hypoxanthine phosphoribosyltransferase (HPRT), and major histocompatibility complex (MHC) class 1.[24] The amplification efficiency of the different PCRs was established on a dilution range of the pooled cDNA. C_t was highly correlated with the

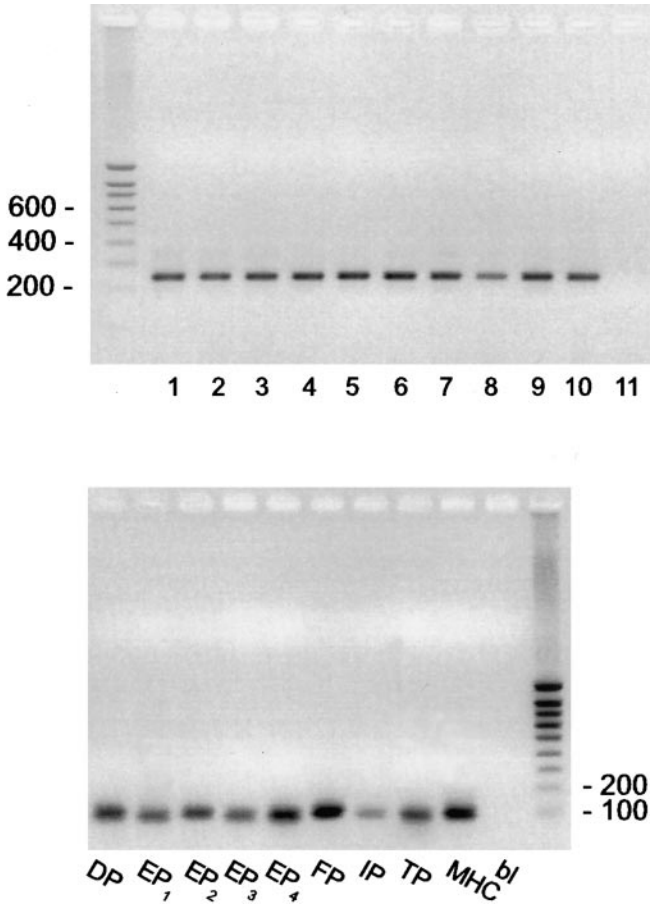

FIGURE 2. *Top*: the results for all 10 TM cDNA samples of a conventional endpoint PCR against actin, using intron-spanning primers. Note the presence of a single band demonstrating the absence of contaminating genomic DNA. *Lane 11*: nontemplate control, using a sample that underwent all procedures, except the presence of isolated TM tissue in the homogenization buffer. *Bottom*: the results of a PCR using the different prostaglandin receptor primer pairs and one housekeeping gene (MHC) on a pooled sample of the 10 TM cDNAs. *Lane bl*: nontemplate control run.

dilution factor. The reaction efficiency (E) was derived from these data for all primer combinations, and all had values close to 2 (Table 3).

The absolute amount (E^{-C_t}) of each housekeeping gene in all individual samples was determined. The mean of the 10

TABLE 3. Amplification Efficiency Constant (E) for the PCRs and Corresponding Correlation Coefficients

PCR	E	R^2
DP	1.91	0.998
EP_1	1.87	0.980
EP_2	1.78	0.973
EP_3	1.89	0.968
EP_4	1.85	0.993
FP	1.92	0.991
IP	1.88	0.996
TP	1.82	0.966
β-actin	1.93	0.997
HPRT	2.00	0.965
MHC class 1	1.99	0.994
GAPDH	2.00	0.999

All curves were based on at least four dilutions of the cDNA each performed in duplicate.

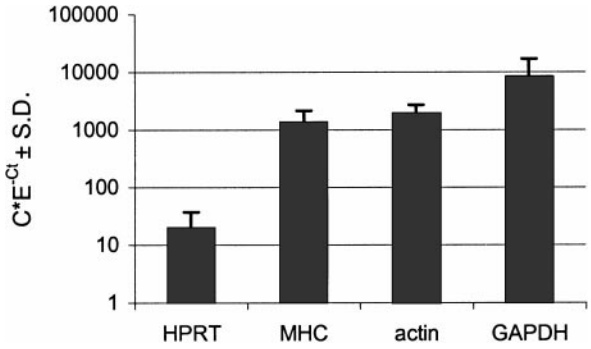

FIGURE 3. Mean levels ± SD of housekeeping genes in the 10 TM cDNA samples. *Vertical axis* is a log scale.

samples is presented in Figure 3. The order of abundance was identical in all 10 TM cDNA samples: HPRT had the lowest abundance; the level of MHC was, on average, 98 times that of HPRT; the level of β-actin was 145 times that of HPRT; and the abundance of GAPDH was 459 times more than that of HPRT. These levels are in agreement with the frequency with which MHC (1×), β-actin (2×), and GAPDH (11×) were encountered in a screening of a human TM cDNA bank.[24] Levels were significantly different from each other (paired Student's t-test; β-actin versus MHC, $P \leq 0.037$; all other comparisons, $P < 0.001$). For all levels of housekeeping genes, there was a trend between age and decreasing amounts present at higher age: HPRT, $R^2 = 0.41$; MHC, $R^2 = 0.35$; β-actin, $R^2 = 0.58$ ($P < 0.02$); GAPDH, $R^2 = 0.58$ ($P < 0.02$). The coefficient of variance (SD/mean · 100%) for the amount of housekeeping genes was 91% for HPRT, 61% for MHC, 45% for β-actin, and 106% for GAPDH. The levels of the housekeeping genes showed a trend for a correlation in expression level among each other ($R^2 = 0.33$–0.87), and the level of variance was indeed reduced by normalization to any of the housekeeping genes within each sample. These results show that the expression profile of the studied housekeeping genes is similar between the samples. However, it must be emphasized that a relatively large variation in the amounts is present, partly explained by the age of the donor, and that normalization to a reference gene has only a limited effect on the variation. We decided to perform the quantitative real-time PCR runs on the prostanoid receptor genes in parallel with a PCR on β-actin, which was selected for use as an optional reference gene for normalization.

The expression profile of the prostanoid receptors and β-actin genes in terms of absolute amounts (Table 4) revealed a rather uniform expression profile in the TM samples. In all samples β-actin was the most abundant (mean amount, 4660) followed in all samples by EP_2 (1674) and at lower levels FP (175), TP (156), EP_4 (136), IP (134), EP_1 (105), DP (40), and EP_3 (9). The levels of β-actin again showed a significant inverse correlation with age ($R^2 = 0.68$; $P < 0.05$; Fig. 4), but the prostanoid receptor levels showed no such correlation. As would be expected from these data, normalizing to the β-actin levels enhanced the coefficient of variation, making such an approach ineffective. For the final analysis, the total expression of the prostanoid receptor genes was calculated (Table 4) and set at 100%. This total did not correlate with age ($R^2 = 0.17$). Subsequently, the relative contributions as a fraction of this total of each prostanoid receptor subtype were determined for each sample. This calculation resulted in a clear reduction of the coefficient of variation. The outcome of this analysis is presented in Figure 5. Statistical analysis showed significant differences in expression between EP_3 and DP (0.4% ± 0.2% [mean ± SD] vs. 1.8% ± 0.7%; $P < 0.00001$, paired Student's

TABLE 4. Absolute Expression Levels ($C \cdot E^{-Ct}$) of β-Actin, Prostanoid Receptor Subtypes, and the Total Expression of All Prostanoid Receptor Subtypes

	β-Actin	DP	EP_1	EP_2	EP_3	EP_4	FP	IP	TP	Total Receptors
1	3783	106	275	3057	33	427	429	380	443	5150
2	1909	25	74	893	5	87	97	88	37	1305
3	3935	39	116	1009	10	175	187	164	226	1927
4	9353	57	145	2970	10	202	300	164	231	4080
5	4937	13	31	475	4	33	39	56	76	726
6	7018	51	169	2894	7	113	212	123	221	3790
7	6550	36	98	2820	9	154	187	102	110	3516
8	1249	35	75	529	7	81	146	99	96	1068
9	4357	30	51	1445	5	57	96	83	100	1866
10	3507	9	19	646	2	36	55	85	22	875
Mean ± SD	4660 ± 2430	40 ± 28	105 ± 76	1674 ± 1121	9 ± 9	136 ± 117	175 ± 119	134 ± 93	156 ± 127	2430 ± 1569
CV (%)	52	69	72	67	95	86	68	69	81	65

CV, coefficient of variation.

t-test), DP and EP_1 (1.8% ± 0.7% vs. 4.4% ± 1.6%; $P < 0.00003$), and EP_1 and EP_4 (4.4% ± 1.6% vs. 5.6% ± 2.2%; $P < 0.024$). The levels of EP_4 (5.6% ± 2.2%), IP (6.4% ± 2.6%), TP (6.5% ± 3.3%), and FP (7.4% ± 2.7%) were not significantly different from each other. The EP_2 levels (67.6% ± 10.7%) were, on average, 10 times of that of FP, a highly significant difference from all other prostanoid receptors ($P < 0.00001$).

DISCUSSION

The main result of this study using quantitative real-time PCR was the finding that all the cloned prostanoid receptors were expressed in human TM tissue in a reproducible pattern that was observed in all samples. The expression profile shows differential gene expression levels with the EP_2 receptor–encoding transcript present in the highest abundance, followed by FP, TP, IP, and EP_4, at levels that were approximately 10 to 15 times lower than that of EP_2. DP and EP_3 were present at the lower levels, which were on average 45 times and 228 times lower than EP_2, respectively.

Quantitative real-time PCR was performed on random primer–generated cDNA, which allows a greater freedom of primer design that is not limited to the 3′ end of the mRNA. The interpretation of the data in terms of expression levels of different transcripts assumes the same efficiency of the RT reaction for each of the transcripts. This premise is difficult to deal with in a completely satisfactory way, but we obtained similar prostanoid receptor expression profiles from TM cDNA primed with oligo dT (data not shown). Calibration strategies in quantitative real-time PCR often rely on normalization against the levels of a housekeeping gene, and we set out to use this approach. It has been reported that postmortem interval has, at most, only a modest effect on RNA levels[25] and, in line with this view, no effects were found of either enucleation or postmortem interval on prostanoid receptor gene expression. However, for two of the investigated housekeeping genes, β-actin and GAPDH, there was a significant correlation between age and decreasing levels. Age-dependent shifts in specific protein concentration in human TM tissue have been reported, with the decrease of a protein tentatively identified as actin with increasing age.[26] Normalization against our housekeeping gene of choice (β-actin) was ineffective. No correlation with age was found for the prostanoid receptor subtype–encoding genes, and we therefore normalized against the total level of the eight prostanoid receptor genes.

We conclude that the steady state transcript levels of the prostanoid receptor genes are set at different levels, and that the pattern of expression does not alter with age in the range

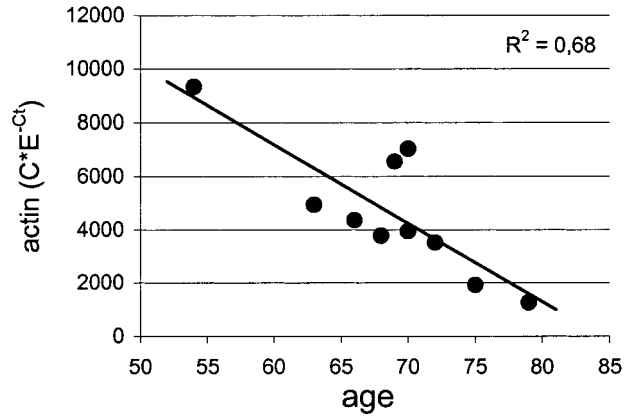

FIGURE 4. Linear correlation between the age of the donor and the amount of β-actin levels in the cDNA sample. Spearman correlation coefficient, $R^2 = 0.68$ ($P < 0.05$).

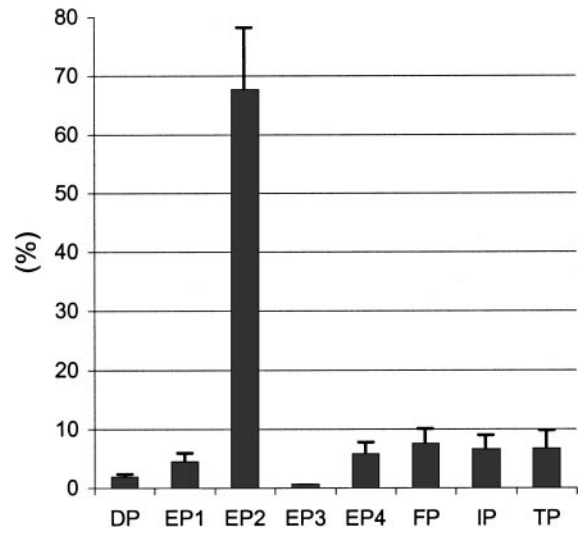

FIGURE 5. Mean ± SD contribution of the prostaglandin receptor subtypes to the total expression level of the prostanoid receptors set at 100%. Statistical analysis with paired Student's *t*-test showed significant differences in expression between EP_3 and DP ($P < 0.00001$), DP and EP_1 ($P < 0.00003$), and EP_1 and EP_4 ($P < 0.024$). The levels of EP_4, IP, TP, and FP were not significantly different from each other. The EP_2 levels (67.6%) were, on average, 10 times of that of FP ($P < 0.00001$).

included in our study (54–79 years). Because the gene expression of the EP_2 receptor was, on average, 15 times (range, 6–25) more than that of the EP_4 receptor, it may be concluded that the increase in flow and cAMP levels in response to the activation of the EP receptors by application of PGE_1 is primarily mediated by the EP_2 receptor.[16] The relatively high expression levels in the TM of EP_2 mRNA compared with EP_4 mRNA in the TM may be an exceptional situation, because in most tissues of the mouse, EP_2 mRNA is expressed at much lower levels than EP_4 mRNA, which may be related to the fact that the TM is a nonvascularized tissue.[27] It is also interesting to note that the EP_4 receptor was sensitive for agonist-induced desensitization, but that the EP_2 receptor was not—a physiological difference that may be of importance for designing pharmacologic intervention strategies to improve outflow through the TM.[28]

The presence in the TM of several prostanoid receptors has been shown by using different morphologic techniques. Immunoreactivity against the EP_2 and EP_3 receptors has been localized in porcine TM,[17] and the EP_3 receptor has been detected in human TM.[4] Immunoreactivity and in situ hybridization have shown the presence of FP in monkey[18] and human TM.[19] A preliminary report on the immunolocalization of EP_1 through EP_4 and FP describes the expression of all these receptors in human TM.[29] Recently, the pharmacologic profile of the prostanoid receptors positively coupled to stimulation of cAMP levels in immortalized cultured human TM cells has been described.[30] Butaprost, a selective EP_2 receptor agonist, is the most potent and efficacious. Because the PGE_2-mediated response is inhibited by 20% by the EP_4-specific receptor antagonist AH23848B, a small contribution of EP_4 receptors is implied.[30] This pharmacologic result corroborates our finding of the predominant contribution of the EP_2 receptors to the prostanoid receptors positively coupled to adenylyl cyclase. In the same study, DP and IP receptor agonists were weak or inactive,[30] and to our knowledge, no reports have been published on the localization of DP or IP in TM. Nevertheless, in our current results both genes were expressed in TM. The gene expression of the IP receptor indicates that prostacyclin or prostacyclin analogues may also exert an effect on human TM function by raising the cAMP levels. Topical application of iloprost, a stable prostacyclin analogue, reduces the IOP in rabbits and beagles and increases tonographic outflow facilitation in rabbits.[8]

Functional tests on isolated bovine TM strips have provided additional insight regarding which of the prostanoid receptors is present in this tissue. A relaxing effect of AH13205, an EP_2 receptor agonist, has been described that may be related to the described effect of PGE_1 on outflow enhancement.[16,20] In contrast, activation of TP receptors induces a contraction of TM.[20,21] Although an extrapolation of PCR data to the protein level has to be made with restraint, the results described herein indicate that the density of the EP_2 receptors, with a relaxant flow-enhancing effect, dominates the contraction-mediating TP receptors.

The ocular hypotensive effect of FP receptor agonists ($PGF_{2\alpha}$ and latanoprost) is well known. Their effect is based on the increase of flow through the uveoscleral route, with a small effect on the outflow through the TM.[31,32] It has been suggested that the activation of the FP and EP_2 receptors in the ciliary muscle leads to cAMP formation, protein kinase activation, and the induction of transcription factors. These responses lead to an increased synthesis of various matrix metalloproteinases (MMPs) and a reduction of extracellular matrix resistance in the uveoscleral outflow pathway.[31] However, in the anterior chamber perfusion model, the ciliary muscle is not present, and $PGF_{2\alpha}$ has no detectable effect on the flow or cAMP production within the time frame of several hours during which we observed the outflow.[16,33,34] In addition, $PGF_{2\alpha}$ did not increase adenylyl cyclase activity in membrane fractions of human TM, whereas PGE_1 and PGE_2 did.[33] This indicates that an activation of FP receptors, implicated from our PCR data and morphologic studies to be present in the TM,[18,19,29] will probably lead to the activation of the phospholipase C pathway, but this does not seem to result in a rapid increase of TM outflow. The precise localization in the human TM and the function of the FP receptors in this tissue remains to be established.

In conclusion, our studies have provided a characterization of the gene expression profile of the different prostanoid receptor genes in the human TM. The predominant presence of EP_2 receptor transcript may provide a basis for a better understanding of the effects of prostaglandin receptor agonists and antagonist on the outflow of aqueous humor through the TM and the regulation of IOP in glaucoma.

Acknowledgments

The authors thank the collaborators at the Cornea Bank, Amsterdam, for their crucial contribution.

References

1. Lütjen-Drecoll E. Functional morphology of the trabecular meshwork in primate eyes. *Prog Retinal Eye Res.* 1998;18:91–119.
2. Francis BA, Alvarado J. The cellular basis of aqueous outflow regulation. *Curr Opin Ophthalmol.* 1997;8:19–27.
3. Hoyng PFJ, Van Beek LM. Pharmacological therapy for glaucoma: a review. *Drugs.* 2000;59:411–434.
4. Woodward DF, Regan JW, Lake S, Ocklind A. The molecular biology and ocular distribution of prostanoid receptors. *Surv Ophthalmol.* 1997;41:S15–S21.
5. Camras CB, Alm A, Watson P, Stjernschantz J. Latanoprost, a prostaglandin analog, for glaucoma therapy: efficacy and safety after 1 year of treatment in 198 patients. Latanoprost Study Groups. *Ophthalmology.* 1996;103:1916–1924.
6. Rulo AH, Greve EL, Hoyng PF. Additive effect of latanoprost, a prostaglandin $F_{2\alpha}$ analogue, and timolol in patients with an elevated intraocular pressure. *Br J Ophthalmol.* 1994;78:899–902.
7. Lindén C, Alm A. Prostaglandin analogues in the treatment of glaucoma. *Drug Aging.* 1999;14:387–398.
8. Hoyng PF, De Jong N. Iloprost, a stable prostacyclin analog, reduces intraocular pressure. *Invest Ophthalmol Vis Sci.* 1987;28:470–476.
9. Bhattacherjee P, Williams BS, Paterson CA. Responses of intraocular pressure and the pupil of feline eyes to prostaglandin EP_1 and FP receptor agonists. *Invest Ophthalmol Vis Sci.* 1999;40:3047–3053.
10. Wang R-F, Lee P-Y, Podos SM, Serle JB, Becker B. Effect of 8-iso prostaglandin E_2 on aqueous humor dynamics in monkeys. *Arch Ophthalmol.* 1998;116:1213–1216.
11. Waterbury LD, Eglen RM, Taurot GF, Cooper GF. EP_3, but not EP_2, FP, or TP prostanoid-receptor stimulation may reduce intraocular pressure. *Invest Ophthalmol Vis Sci.* 1990;31:2560–2567.
12. Woodward DF, Hawley SB, Williams LS, et al. Studies on the ocular pharmacology of prostaglandin D_2. *Invest Ophthalmol Vis Sci.* 1990;31:138–146.
13. Breyer RM, Bagdassarian CK, Myers SA, Breyer MD. Prostanoid receptors: subtypes and signaling. *Annu Rev Pharmacol Toxicol.* 2001;41:661–690.
14. Polansky JR, Kurtz RM, Alvarado JA, Weinreb RN, Mitchell MD. Eicosanoid production and glucocorticoid regulatory mechanisms in cultured human trabecular meshwork cells. *Prog Clin Biol Res.* 1989;312:113–138.
15. Coleman RA, Smith WL, Narumiya S. VIII. International union of pharmacology classification of prostanoid receptors: properties, distribution, and structure of the receptors and their subtypes. *Pharmacol Rev.* 1994;46:205–229.

16. Dijkstra BG, Schneemann A, Hoyng PF. Flow after prostaglandin E_1 is mediated by receptor-coupled adenylyl cyclase in human anterior segments. *Invest Ophthalmol Vis Sci.* 1999;40:2622–2626.
17. Zhao C, Fujimoto N, Shichi H. Immunocytochemical localization of prostaglandin E2 receptor subtypes in porcine ocular tissues. I: uveal tissues. *J Ocul Pharmacol Ther.* 1995;11:421–435.
18. Ocklind A, Lake S, Wentzel P, Nistér M, Stjernschantz J. Localization of the prostaglandin $F_{2\alpha}$ receptor messenger RNA and protein in the cynomolgus monkey eye. *Invest Ophthalmol Vis Sci.* 1996; 37:716–726.
19. Anthony TL, Pierce KL, Stamer WD, Regan JW. Prostaglandin $F_{2\alpha}$ receptors in the human trabecular meshwork. *Invest Ophthalmol Vis Sci.* 1998;39:315–321.
20. Krauss AH, Wiederholt M, Woodward DF. Prostaglandin effects on the contractility of bovine trabecular meshwork and ciliary muscle. *Exp Eye Res.* 1997;64:447–453.
21. Wiederholt M, Thieme H, Stumpff F. The regulation of trabecular meshwork and ciliary muscle contractility. *Prog Retinal Eye Res.* 2000;19:271–295.
22. Bustin SA. Absolute quantification of mRNA using real-time reverse transcription polymerase chain reaction assays. *J Mol Endocrinol.* 2000;25:169–193.
23. Meijerink J, Mandigers C, van De Locht L, Tonnissen E, Goodsaid F, Raemaekers J. A novel method to compensate for different amplification efficiencies between patient DNA samples in quantitative real-time PCR. *J Mol Diagn.* 2001;3:55–61.
24. Gonzalez P, Epstein DL, Borrás T. Characterization of gene expression in human trabecular meshwork using single-pass sequencing of 1060 clones. *Invest Ophthalmol Vis Sci.* 2000; 41:3678–3693.
25. Barton AJL, Pearson RCA, Najlerahim A, Harrison PJ. Pre- and postmortem influences on brain RNA. *J Neurochem.* 1993;61:1–11.
26. Millard CB, Tripathi BJ, Tripathi RC. Age-related changes in protein profiles of the normal human trabecular meshwork. *Exp Eye Res.* 1987;45:623–631.
27. Katsuyama M, Nishigaki N, Sugimoto Y, et al. The mouse prostaglandin E receptor EP_2 subtype: cloning, expression, and northern blot analysis. *FEBS Lett.* 1995;372:151–156.
28. Nishigaki N, Negishi M, Ichikawa A. Two Gs-coupled prostaglandin E receptor subtypes, EP_2 and EP_4, differ in desensitization and sensitivity to the metabolic inactivation of the agonist. *Mol Pharmacol.* 1996;50:1031–1037.
29. Schloetzer-Schrehardt UM, Nuesing RM, Naumann GOH. Immunolocalization of prostaglandin E_2 and F_2 alpha receptor proteins in human ocular tissues. *Invest Ophthalmol Vis Sci.* 2000;41(4):**S**250. Abstract nr 1315.
30. Crider JY, Sharif NA. Functional pharmacological evidence for EP_2 and EP_4 prostanoid receptors in immortalized human trabecular meshwork and non-pigmented ciliary epithelial cells. *J Ocul Pharmacol Ther.* 2001;17:35–46.
31. Schachtschabel U, Lindsey JD, Weinreb RN. The mechanisms of action of prostaglandins on uveoscleral outflow. *Curr Opin Ophthalmol.* 2000;11:112–115.
32. Mishima HK, Kiuchi Y, Takamatsu M, Racz P, Bittigau P. Circadian intraocular pressure management with latanoprost: diurnal and nocturnal intraocular pressure reduction and increased uveoscleral outflow (review). *Surv Ophthalmol.* 1997;41:S139–S144.
33. Dijkstra BG, Ruijter JM, Hoyng PF. Outflow characteristics of isolated anterior segments of human eyes. *Invest Ophthalmol Vis Sci.* 1996;37:2015–2021.
34. Busch MJWM, Kobayashi K, Hoyng PFJ, Mittag TW. Adenylyl cyclase in human and bovine trabecular meshwork. *Invest Ophthalmol Vis Sci.* 1993;34:3028–3034.
35. Ten Hulzen RD, Johnson DH. Effect of fixation pressure on juxtacanalicular tissue and Schlemm's canal. *Invest Ophthalmol Vis Sci.* 1996;37:114–124.